International Journal of Engineering & Technology, 7 (3.17) (2018) 145-150

International Journal of Engineering & Technology

Website: www.sciencepubco.com/index.php/IJET

Research paper

Modeling, Simulation and Analysis of Induction Motor for Electric Vehicle Application

Yushaizad Yusof[1]* and Kamarulzaman Mat[2]

[1]*INTEGRA*
[2]*PAKET*
Faculty of Engineering and Built Environment
43600 UKM Bangi, Malaysia
**Corresponding author Email: yushaizad@ukm.edu.my*

Abstract

High power induction motor (IM) is widely used in industries and recently has been put into electric vehicle as the replacement of the internal combustion engine. In order to study the characteristics of the IM, a model of three-phase squirrel cage induction motor is designed and developed using MATLAB Simulink tool. Synchronous reference frame (SRF) technique is implemented to simplify the equivalent circuit model. Based on state space form, a flux linkage equation is developed using three stages transformation matrices. It demonstrated a good performance with fast response for AC start-up test, where simulated induced torque, rotor speed, mechanical output power, efficiency, slip and stator current waveforms were generated accordingly. Indeed, the developed IM model can be used as a starting platform to further study and analyses the IM drives performance for electric vehicle application.

Keywords: *Induction motor, Synchronous reference frame, Electric vehicle, MATLAB Simulink, Flux linkage*.

1. Introduction

Electric vehicles (EVs) such as electric car, electric train etc. contribute in mitigating significant environmental issues such as air pollution, global warming etc. due to gas emission from gasoline-powered vehicles with internal combustion engines (ICE) [1]. In general, the EVs can be categorized into battery-based electric vehicle (BEV) or hybrid electric vehicle (HEV) [2]. Apart from energy efficiency and lower gas emission, other advantage of the EV is the availability of electric energy through electric distribution systems, especially in urban areas. Typical disadvantages are low energy density and longer charging time for the present batteries such as Li-ion battery, lead acid battery etc. [3]. Optimal energy management is very important to be investigated in the EVs; in addition to optimum design of the motor, selection of a proper drive, and optimal control strategy of the EVs propulsion system.

Type of propulsion systems reported in literature and usually selected for EVs are internal permanent magnet motor (IPM), brushless DC motor (BLDC), permanent magnet synchronous motor (PMSM) and induction motor (IM) [4]. Basically, a desired features of the propulsion system for EVs are high ratio of torque to inertia and power to weight, high maximum torque capability, high speed, low level of audible noise, low maintenance, small size, low weight, reasonable cost, high efficiency over low and high-speed ranges, energy recovery on braking, and non-sensitivity to acceleration forces [5]. An electromechanical motor is considered as the workhorse of EVs. Its basic function is to convert electrical energy supplied by the battery to mechanical energy which drives the vehicle. Squirrel-cage type IM has many of the abovementioned features as well as it is inexpensive and eases of availability. Moreover, this type of IM is widely used in the industry due to its robustness, reliability and ease of control technique. A comparative study between aforementioned propulsion systems above, found that the IM fulfils major requirement of the HEV propulsion system [4].

Basically, the IM consists of a stator (the fixed part) and a rotor (the moving part) separated by an air gap [6]. The stator contains electrical windings housed in axial slots. Each phase on the stator has distributed winding, consisting of several coils distributed in a number of slots. The distributed winding results in magnetomotive forces (MMF) due to the current in the winding with a stepped waveform similar to a sine wave. In a three-phase machine the three windings have spatial displacement of $2\pi/3$ radian between them. When a balanced three-phase currents applied, the resultant MMF in the air gap produces constant magnitude and rotates at base angular speed of $\omega_b = 2\pi f_b$ (rad/s) where f_b is the base frequency in Hz. The actual speed rotation of magnetic field depends on the number of poles, p and f_b. This speed is known as synchronous speed, n_s and usually measured in revolution per minute (rpm) and is expressed as,

$$n_s = \frac{120 f_b}{p} \text{ (rpm)} \tag{1}$$

The magnetic field or stator flux, λ_s has uniform strength and travels at angular speed, equals to its stator frequency. The magnetic field induces electromagnetic force (EMF), E in the rotor windings. As the rotor windings are short-circuited, the circulating currents generate a reaction. Based on Lenz's law, the reaction is used to counter the source of rotor current (induced EMF in the rotor), in turn, the rotor rotating magnetic field itself. The induced EMF will be countered if the difference in the speed of stator's rotating magnetic field and the rotor's becomes zero. The rotor

turning in the same direction as the stator magnetic field and catch up with it eventually. Depending on the load connected to the shaft, the rotor speed n_r, is always smaller than the stator speed, n_s. The difference between both speeds is called the slip speed, n_{sl}, while n_m denotes a mechanical speed. Hence, the n_{sl} can be expressed as,

$$n_{sl} = n_s - n_r = n_s - \frac{p}{2} n_m \text{ (rpm)} \quad (2)$$

$$s = \frac{n_{sl}}{n_s} = \frac{n_s - n_r}{n_s} \quad (3)$$

Equation (3) defines slip *s*, a ratio of n_{sl} and n_s.

In EV, the IM is connected in between the power source (stacks of batteries) and the car's chassis, interfaced by the motor controller similar to Figure 1[6]. The motor controller mainly comprises of an inverter circuit and a control unit. It is essential to understand its parameters, construction, mathematical representation and working principle. Normally, the study on IM is carried out by employing computer assisted simulation and modeling tools like MATLAB Simulink software. The MATLAB Simulink based IM models are available in the literatures [7-10]. It models, simulates and analyses dynamic systems such as transient and steady state responses of the IM. To model the IM, mathematical representation based on state space representation or transfer function are employed, derived and arranged to form a complete set of motor model [7-9]. Indeed, the understanding on the basic IM operation such as motor start up and load's characteristics through computer modelling and simulation, is very important and will inspire high performance IM drive system design for EV application. Therefore, as a preliminary study, this paper begins with the design of IM model, followed by the discussion of the simulation results and finally, closed by the concluding remarks.

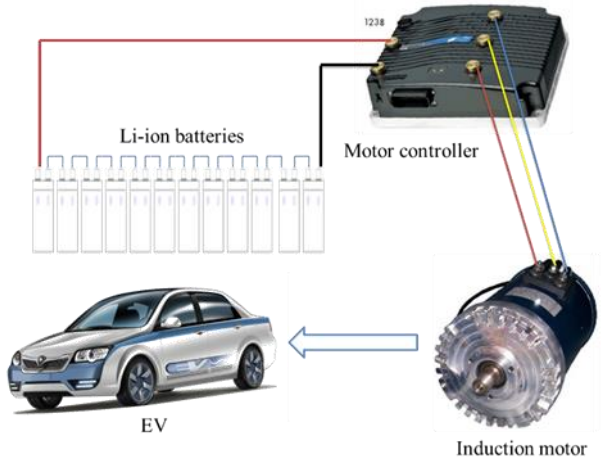

Fig.1: Electric propulsion system connection in EV

2. Induction Motor Dynamic Model

The following assumptions are made to develop IM model [11]:

- The magnetic circuit is linear.
- The iron losses are neglected.
- The mechanical losses are neglected.

In order to simplify the derivation of induction motor's mathematical expression; a direct-quadrature (*d*-*q*) approach was implemented based on the model derived from equivalent circuit [8]. Figure 2 shows the equivalent circuit model for the IM in synchronous reference frame.

2.1. Nomenclature

$\boldsymbol{A}$	system matrix
$\boldsymbol{B}$	input matrix
u	scalar input
$\boldsymbol{x}$	state variable
d	direct axis
q	quadrature axis
s	stator variable or slip
r	rotor variable
α-β	alfa-beta axis
V_{ds} (V_{qs})	d-axis (q-axis) stator voltages
i_{ds} (i_{qs})	d-axis (q-axis) stator current
i_{dr} (i_{qr})	d-axis (q-axis) rotor current
$I_{n,rms}$	n^{th} rms current
ψ_{ds} (ψ_{qs})	d-axis (q-axis) stator flux linkages
ψ_{dr} (ψ_{qr})	d-axis (q-axis) rotor flux linkages
λ_{ds} (λ_{dr})	Stator (rotor) flux
R_s (R_r)	Stator (rotor) resistance
L_s (L_r)	Stator (rotor) inductance
L_m	Magnetizing inductance
L_{ls} (L_{lr})	Stator (rotor) leakage inductance
X_{ls}	Stator leakage reactance
X_{lr}	Rotor leakage reactance
X_m	Mutual reactance
X_{ml}	Mutual leakage reactance
E	Electromotive force
ω_e (ω_r)	Stator (rotor) electrical angular frequency
ω_b	Motor electrical angular base frequency
ω_{slip}	Slip frequency
f_b	Base frequency
n_s	Synchronous speed
n_r	Rotor speed
n_m	Mechanical speed
θ_e	Phase angle
p	Poles number
J	Moment of inertia
P_o	Consumed (output) power
P_{in}	Developed (input) power
η	Efficiency
T_{em}	Electrical output torque
T_L	Load torque
t	Time function

2.2. State Equation Of IM

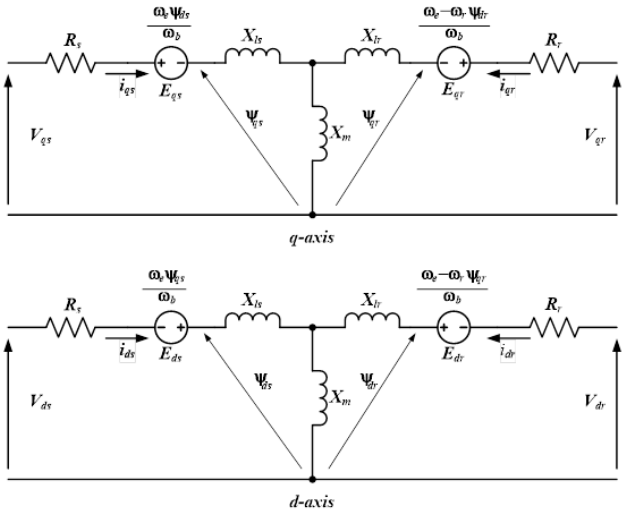

Fig.2: Equivalent circuit of IM in SRF

By using the mathematical expression of IM dynamic model based on SRF presented in [7-9], the model of IM is designed. Therefore, the stator and rotor voltages equations are:

$$v_{qs} = \frac{p}{\omega_b} F_{qs} + \frac{\omega_e}{\omega_b} F_{ds} + r_s i_{qs} \quad (5)$$

$$v_{ds} = \frac{p}{\omega_b}F_{ds} + \frac{\omega_e}{\omega_b}F_{qs} + r_s i_{ds} \quad (6)$$

$$v_{qr} = \frac{p}{\omega_b}F_{qr} + \left(\frac{\omega_e - \omega_r}{\omega_b}\right)F_{dr} + r_s i_{qr} \quad (7)$$

$$v_{dr} = \frac{p}{\omega_b}F_{dr} + \left(\frac{\omega_e - \omega_r}{\omega_b}\right)F_{qr} + r_s i_{dr} \quad (8)$$

Before the rotating SRF based stator voltage is implemented, the three-phase voltage quantity is transformed into two-phase SRF in three stages, namely an isolated neutral system, a Clarke and a Park transformation in sequence. The steps of transformation is depicted in Figure 3. To revert back from SRF system into three-phase system, an inverse Park and an inverse Clarke transformation matrices is to be used.

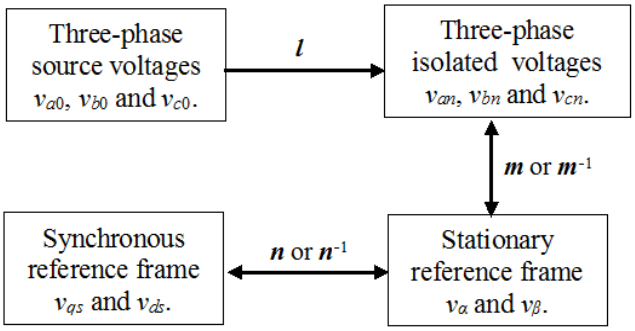

Fig. 3: Voltage transformation process

where, $\boldsymbol{l}$: phase to isolated neutral system transformation; $\boldsymbol{m}$: Clarke transformation and $\boldsymbol{n}$: Park transformation respectively. Hence,

$$\boldsymbol{v_{sn}} = \begin{bmatrix} V_m \sin \omega t \\ V_m \sin(\omega t - 2\pi/3) \\ V_m \sin(\omega t + 2\pi/3) \end{bmatrix} \quad (8)$$

$$\boldsymbol{l} = \begin{bmatrix} 2/3 & -1/3 & -1/3 \\ -1/3 & 2/3 & -1/3 \\ -1/3 & -1/3 & 2/3 \end{bmatrix} \quad (9)$$

$$\boldsymbol{m} = \begin{bmatrix} 1 & 0 & 0 \\ 0 & -1/\sqrt{3} & 1/\sqrt{3} \end{bmatrix} \quad (10)$$

$$\boldsymbol{n} = \begin{bmatrix} \cos\theta_e & -\sin\theta_e \\ \sin\theta_e & \cos\theta_e \end{bmatrix} \quad (11)$$

The relation between flux linkage, ψ and the flux, λ is given by the following expression:

$$\Psi = \omega_b \lambda \text{ (V)} \quad (12)$$

Based on SRF, the IM dynamic model can be represented in state equation [11]. Generally, the IM model can be divided into electrical and mechanical parts respectively. Thus, for the electrical part, it represents ψ as the state variables and stator voltages in SRF, v_{qs} and v_{ds} as the inputs. Hence,

$$\dot{\boldsymbol{x}} = \boldsymbol{Ax} + \boldsymbol{Bu} \quad (13)$$

$$\begin{bmatrix} \dot{\Psi}_{qs} \\ \dot{\Psi}_{ds} \\ \dot{\Psi}_{qr} \\ \dot{\Psi}_{qs} \end{bmatrix} = \begin{bmatrix} a_{11} & -\omega_e & a_{13} & 0 \\ \omega_e & a_{22} & 0 & a_{24} \\ a_{31} & 0 & a_{33} & \omega_r - \omega_e \\ 0 & a_{42} & \omega_e - \omega_r & a_{44} \end{bmatrix} \begin{bmatrix} \Psi_{qs} \\ \Psi_{ds} \\ \Psi_{qr} \\ \Psi_{dr} \end{bmatrix} + \boldsymbol{Bu} \quad (14)$$

where,

$$a_{11} = a_{22} = \omega_b \left(\frac{R_s X_{ml} - R_s}{X_{ls}^2}\right)$$

$$a_{33} = a_{44} = \omega_b \left(\frac{R_s X_{ml} - R_s}{X_{lr}^2}\right)$$

$$a_{13} = a_{24} = a_{31} = a_{42} = \omega_b \frac{R_s X_{ml}}{X_{ls} X_{lr}}$$

$$\boldsymbol{u} = [v_{qs} \quad v_{ds} \quad 0 \quad 0]$$

$$\boldsymbol{B} = \begin{bmatrix} \omega_b \\ \omega_b \\ 0 \\ 0 \end{bmatrix}$$

Mechanical outputs such as consumed torque, T_{em} and rotor speed, ω_r are the product of IM, hence, the expression for both are:

$$T_{em} = \frac{3p}{4\omega_b}\left(\Psi_{ds} i_{qs} - \Psi_{qs} i_{ds}\right) \text{ (Nm)} \quad (15)$$

$$\frac{d\omega_r}{dt} = \frac{2J}{p}(T_{em} - T_L) \quad (16)$$

Three mathematical expressions for the input power P_i, the consumed power P_o, as well as the efficiency, η are given as follows:

$$P_i = 3V_{s,rms} I_{s,rms} \cos\theta_e \text{ (W)} \quad (17)$$

$$P_o = T_{em}\omega_r \text{ (W)} \quad (18)$$

$$\eta = \frac{P_o}{P_i} \quad (19)$$

where cos θ_e represents the power factor.

A total harmonic distortion (THD_i) of stator current is considered for the developed IM model. THD_i measures a quality of current supplies to the IM and the current harmonics drawn by the load. Current harmonics waveform could be characterized from its shape and frequencies that is higher than the fundamental 50 Hz frequency. It is demonstrated by a periodical signal but deviated from pure sinusoidal waveform with significant phase shift. According to IEEE 519 standard [13], the allowable value of THD_i should be less than 5 percent. THD_i greater than 5 percent is not recommended in power system and should be compensated. Therefore, to estimate multiple frequency harmonics magnitude, the following expression is used to calculate the THD_i:

$$\text{THD}_\text{i} = \frac{\sqrt{\sum_{n\neq 1}^{\infty} I_{n,rms}}}{I_{1,rms}} \quad (20)$$

where n = 1, 2, 3, …..

The IM model was designed with three-phase stator voltages and load torque as the inputs, whereby six parameters have been chosen as the outputs. This model is configured using MATLAB Simulink depicted in Figure 4 and Figure 5. Figure 4 shows a block diagram represents the IM with its outputs connected to the scopes. The detail of the IM components connection illustrated in Figure 5, was constructed using interconnection of some basic block diagrams provided by MATLAB Simulink library browser. With respect to stator voltage, v_{qr} and v_{dr} were set to zero. The simulation was run for 0.4 seconds using fixed-step discrete solver. The step time for simulation was 5 μ seconds. The parameters of IM used in simulation is listed in Table 1.

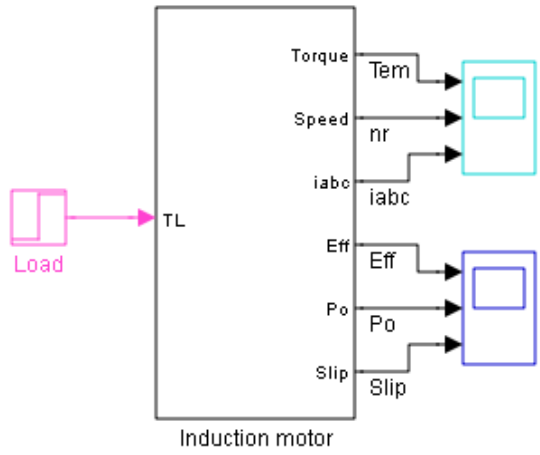

Fig. 4: IM model in MATLAB Simulink environment

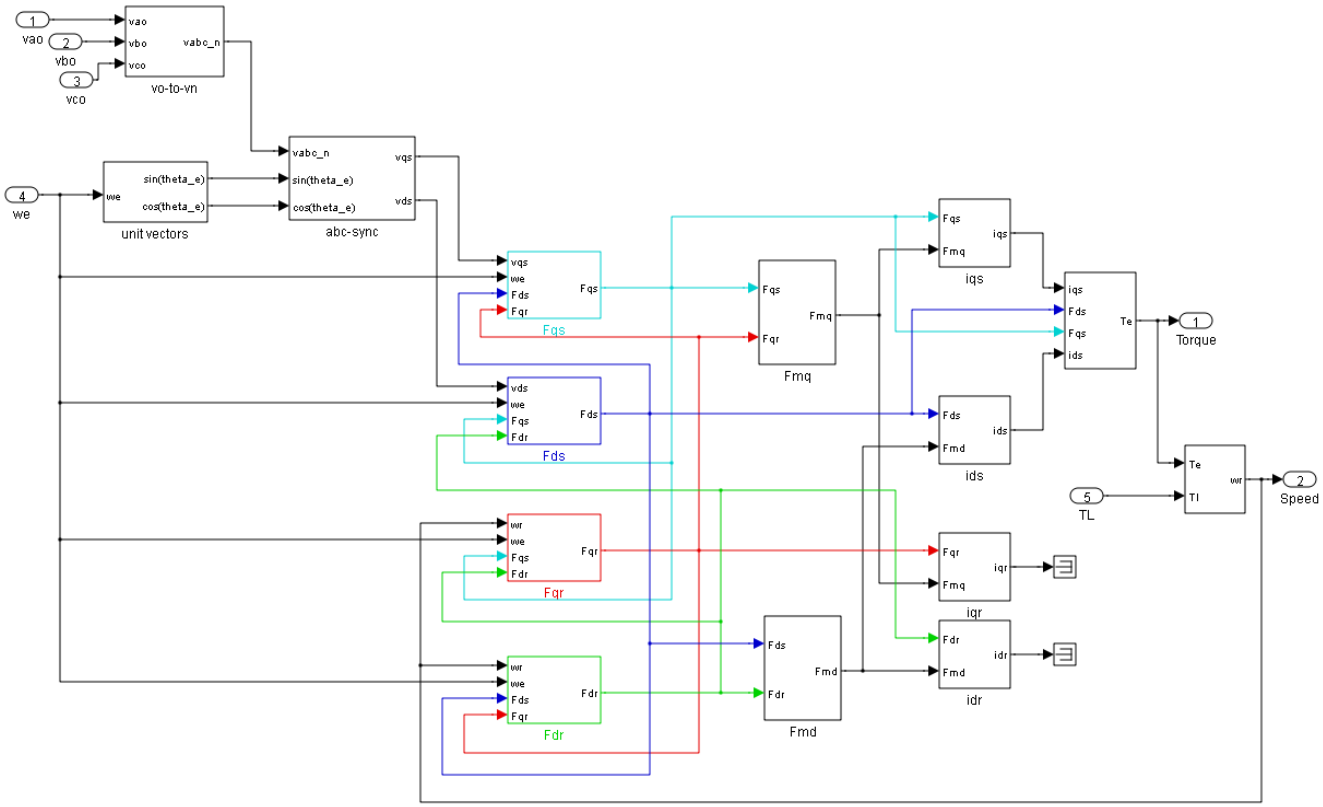

Fig. 5: Model of IM based on flux linkage calculation

Table 1: IM parameters used in simulation

Parameter	Value
Source voltage amplitude, V_m	100 V
Base frequency, f_b	100 Hz
Stator inductance, L_{ls}	0.2 mH
Rotor inductance,L_{lr}	0.6 mH
Magnetizing inductance, L_m	4 mH
Stator resistance, r_s	0.2 Ω
Rotor resistance, r_r	0.4 Ω
Poles, p	4
Inertia, J	0.026 kgm^2

3. Results and Discussion

In order to validate the IM model employing the parameters given in Table 1, it is simulated for AC start-up test. The results of simulation are depicted from Figure 6 to Figure 9. Note that the results show several IM outputs against time. Starts from 0 to 0.2 seconds (equivalent to 10 cycles of AC voltage), no load torque is applied to the IM. After that until the end of simulation (0.4 seconds), the step load torque of 50 Nm was applied. Some significant changes are observed when the load torque increased instantaneously. On the other hand, Figure 9 shows stator current harmonics spectrum, which quantifies the current magnitude of some odd harmonics order up to 20th harmonic order.

3.1. AC Start-Up Test

As shown in the middle trace of Figure 6, the two-phase stator voltage in stationary reference frame (α-β) has been transformed from three-phase stator voltage indicated at top trace. This is done using (9) and (10). Further, it was transformed into synchronously rotating reference frame using (11). Thus, the magnitude of v_{qs} is zero and v_{ds} is 100 V respectively, as depicted in the bottom trace. Therefore, the implemented transformation matrices has successfully transform a three-phase into two-phase voltages, rotating at synchronous reference frame. This is the first step before the state equation is derived.

Depicted in Figure 7 is some outputs obtained from the AC start-up test for the developed IM model. The top trace shows the induced electrical torque, T_{em} where at the beginning an overshoot of 150 Nm is observed before it gradually decreased to zero at 0.1 seconds. However, when the T_L is increased to 50 Nm suddenly, the T_{em} also follows. It takes only 0.05 seconds to reach that value. Unfortunately, for middle trace, the rotor speed, n_r has the reverse effect. At the moment T_L applied to the IM, n_r slows down from 3000 rpm to 2080 rpm. This shows that at no load, n_r runs freely at 3000 rpm which exactly equal to synchronous speed n_s, while no slip develops at that time. Thus, this is according to (3). On the other hand, for the bottom trace of Figure 7, it indicates the three-phase stator current waveforms. At the instant IM starts to energize, the response of sinusoidal three-phase stator currents, i_{abc} is not convincing since it shows unbalance characteristic with a very high amplitude. This is because due to the transient response at no load where overshoot peak always happens. But after, 0.07 seconds it has settled down at around 53 A. However, after 0.2 seconds it steps up to 70 A in just two cycles. The i_{abc} increment is due to higher T_{em}, hence the torque is proportional to the current is proven.

As depicted in the top trace of Figure 8, the efficiency, η of IM oscillates for a while and it reach its highest value once before becoming 0. This is because of transient response and motor's inertia, J effects. Then, after the insertion of TL, the η improves instantaneously from 0 to 0.74. Thus, at no load the η almost none, unless the external torque is applied. The middle trace indicates the P_o response during AC start-up, with and without T_L. The P_o is stabilized at 10890 W when 50 Nm of T_L is applied. The bottom trace shows slip, s characteristics with and without T_L at AC start-up. Obviously, there is no s when T_L is not applied. However, the s maintains at 0.3 after T_L insertion to the IM model.

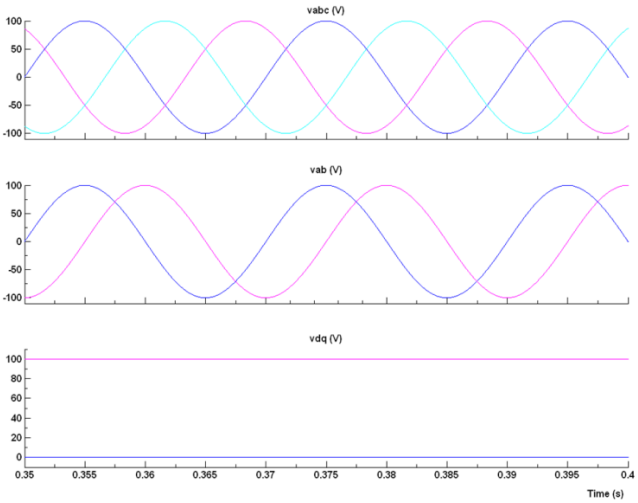

Fig. 6: (From top to bottom) V_{abc}, V_{ab} and V_{dq} waveforms against time

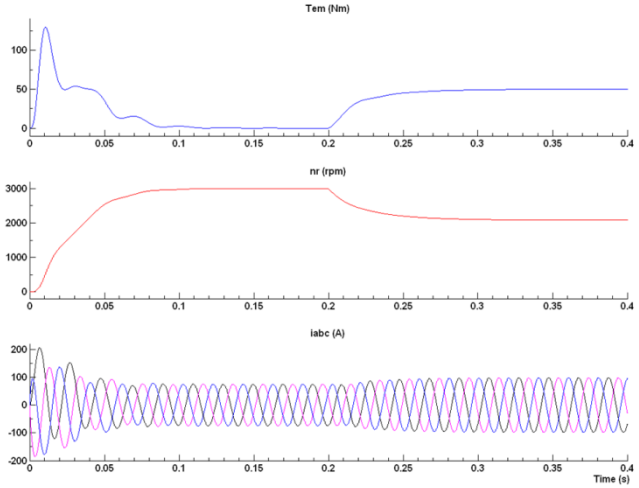

Fig. 7: (From top to bottom) T_{em}, n_r and i_{abc} waveforms against time

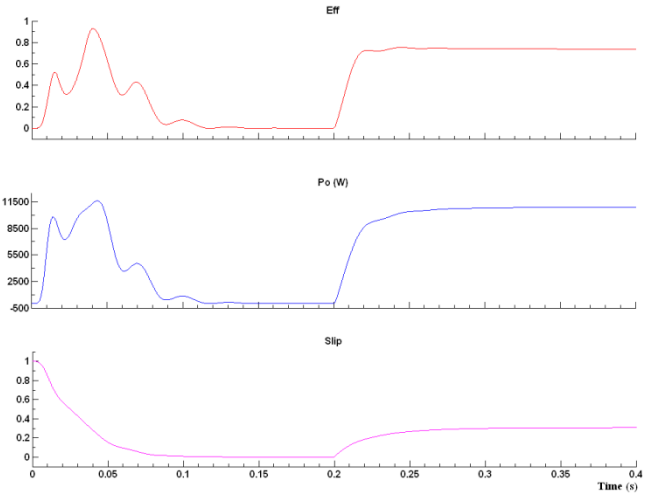

Fig. 8: (From top to bottom) E_{ff}, P_o and Slip waveforms against time

3.2. Stator Currents THD

Determination of stator current THD_i is important in order to measure the quality of supply power. Normally, the IM which is categorized as nonlinear load will draw significant current harmonics from the AC system. Based on Figure 9, the fundamental rms current for each i_{as}, i_{bs} and i_{cs} are 52.9 A, 53.5 A and 53.8 A respectively. Those values are identical to AC rms current. On the other hand, harmonics rms current for each phase are 0.5 A, 0.9 A and 1.4 A respectively. Using equation (20), the THD_i of i_{as}, i_{bs} and i_{cs} are given in Table 2.

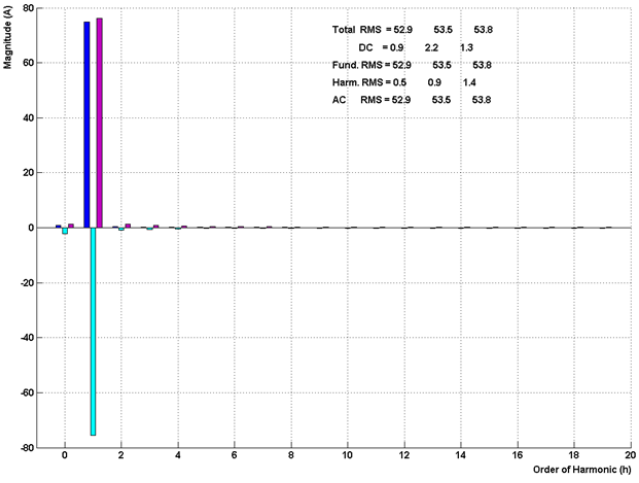

Fig. 9: Harmonic spectrum of stator currents

Table 2: IM parameters used in simulation

	i_{as}	i_{bs}	i_{cs}
THD_i	0.95%	1.68%	2.6%

According to Table 2, all three currents THD_i successfully record an individual value below 5 percent. The measurement of THD_i was taken at steady state condition, but if taken at the start of simulation, the values could be higher since the three-phase stator current waveforms was not purely sinusoidal and unbalance. Based on the result, implies that the quality of power supply to the IM is high, therefore, small losses can be expected.

4. Conclusion

Using a *d-q* transformation, a three-phase voltage can be transformed into two-phase voltage. This is easier to be adjusted and controlled like a DC model or a single-phase model. To realize a *d-q* based SRF, the three-phase system need to have at least two stages of transformation process using equations (9) and (10). But before the three-phase voltage transforms into SRF, it should be changed into phase to neutral form first. Inversely, the IM model will have three-phase system back after the *d-q* system is reverted using Inversed Park and Inversed Clarke transformations matrices.

Based on the results obtained from the simulation indicates significant capability and performance of IM model using MATLAB Simulink tool as the platform to study the IM characteristics. It shows a great potential as the main propulsion for electric vehicle due to its availability, performance and robustness. Depends on load requirement, control technique and the battery management strategy, the IM is expected to be as one of the favourite candidate for the main traction of electric vehicle besides PMSM, IPMM, BLDC etc [14]. With implementation of suitable and advanced motor drive such as vector control and direct torque control, the performance of induction motor drive can be upgraded and improved further [15]. In the future, battery and controller models will be designed and incorporated with the IM model in order to complete the electrical part of the EV system.

Acknowledgement

The authors would like to thank Center of Automobile Research (CAR) and Center of Integrated Engineering and Advanced Technology (INTEGRA), Faculty of Engineering and Built Environment, UKM for the support.

References

[1] Chan, C. C. "The state of art of electric and hybrid vehicles", *Proc. of the IEEE*. Vol. 90, No. 2, (2002), pp. 247-275.

[2] Han, P., Cheng, M. & Chen, Z. "Dual-electrical-port control of cascaded doubly-fed induction machine for EV/HEV applications", *IEEE Trans. Ind. App.*, Vol. 53, No. 2, (2017), pp. 1390-1398.

[3] Yusof, Y., Adnan, M. F. M., Guenther, R., Zaman M. H. M., Ibrahim, A. A. & Ayob, A. "Li-ion battery pack charging process and monitoring in electric vehicle", *Applied Mechanics and Materials*. Vol. 663, (2014), pp. 504-509.

[4] Mounir, Z., Mohamed, E. H. B. & Demba, D. "Electric motor drive selection issues for HEV propulsion systems: a comparative study", *IEEE Trans. Veh. Technol*. Vol. 55, No. 6, (2006), pp. 1756-1764.

[5] Faiz, J., Sharifian, M. B. B., Keyhani, A. & Proca, A. B. "Sensorless direct torque control of induction motors used in electric vehicle", *IEEE Trans. Energy Conv*., Vol. 18, No. 1, (2003), pp. 1-10.

[6] Hassan, N. M., Ali, N. O. and Radzak, M. Y. "Development and installation of battery-powered electric vehicle wiring system", *International Journal of Scientific & Technology Research*, Vol. 3, N0. 11, (2014), pp. 10-15.

[7] Krishnan, R. *Electric motor drives modeling, analysis, and control*. Prentice-Hall Inc., (2001).

[8] Ong, C-M. *Dynamic simulation of electric machinery using MATLAB®/Simulink*. Prentice-Hall Inc., (1998)

[9] Ozpineci, B. & Tolbert, L. M. Simulink implementation of induction machine model – a modular approach. Electric Machines and Drives Conference, 2003. IEMDC'03. IEEE International, Vol. 2, (2003), pp. 728-734.

[10] Haddoun, A., Benbouzid, M. E. H., Diallo, D., Abdessemed, R., Ghouili, J. & Srairi, K. "Modeling, analysis, and neural network control of an EV electrical differential", *IEEE Trans. Energy Conv*., Vol. 18, No. 1, (2008), pp. 1-10.

[11] Stoyanov, L. Implementation of Matlab/Simulink Model of induction motor in students laboratory works – performance characteristics and transient process simulation. 18th International Symposium on Electrical Apparatus and Technologies (SIELA), Burgas, (2014), pp. 1-4.

[12] Lee, R. J., Pillay, P. & Harley, G. "D, Q reference frames for the simulation of induction motors", *Electric Power System Research*, Vol. 8, (1984/85), pp. 15-26.

[13] Yusof, Y. & Rahim, N. A. "Functional simulation model for single phase pulse width modulation-voltage source inverter (PWM-VSI) using switching function concept", *Jurnal Kejuruteraan*, Vol. 23, (2011), pp. 49-56.

[14] Yang, Z., Shang, F., Brown, I. P. & Krishnamurthy, M. "Comparative study of interior permanent magnet, induction, and switched reluctance motor drives for EV and HEV applications", *IEEE Trans. Trans. Elect.*, Vol. 1, No. 3, (2015), pp. 245-254.

[15] Dehghan-Azad, E., Gadoue, S., Atkinson, D., Slater, H., Barrass, P. & Blaabjerg, F. "Sensorless control of IM based on stator-voltage MRAS for limp-home EV applications", *IEEE Trans. Power Electron*., Vol. 33, No. 3, (2018), pp. 1911-1921.